2023-01-01

Artificial eardrum for acoustical test fixtures dedicated to hearing protection assessment

Simon Benacchio
Université de Lille

Yu Luan
ÉTS

Olivier Doutres
ÉTS, Olivier.Doutres@etsmtl.ca

Franck Sgard
IRSST, sgard.franck@irsst.qc.ca

Eleonora Carletti

29th International Congress on Sound and Vibration
The annual congress of the International Institute of Acoustics and Vibration (IIAV)
9–13 July 2023
ICSV29

ARTIFICIAL EARDRUM FOR ACOUSTICAL TEST FIXTURES DEDICATED TO HEARING PROTECTION ASSESSMENT

Simon Benacchio
Arts et Métiers Institute of Technology, LISPEN, HESAM Université, Lille, France
email: simon.benacchio@ensam.eu

Yu Luan, Olivier Doutres
Department of Mechanical Engineering, Ecole de Technologie supérieure, 1100 rue Notre-Dame Ouest, Montréal, Québec H3C 1K3, Canada

Franck Sgard
IRSST, Direction Scientifique, 505 Boulevard de Maisonneuve Ouest, Montréal, Québec, H3A 3C2, Canada

Acoustical test fixtures are commonly used to measure the insertion loss of hearing protectors. For earmuffs, it is known that the tympanic impedance has small effects on the measured attenuation. However, this impedance must be considered for the evaluation of earplugs attenuation. Currently, commercial acoustical test fixtures use standardized ear simulators that reproduce the acoustical behavior of a median human ear. Nevertheless, a previous numerical study has demonstrated that the inter-individual variability of the tympanic impedance observed in the literature can lead to significant variation in the attenuation of an earplug up to 4 kHz. Thus, the use of artificial eardrums that provide several tympanic impedances could be useful to (i) experimentally confirm that the inter-individual variability of the tympanic impedance has an effect on the earplug attenuation and (ii) propose a manner to consider this inter-individual variability during earplug attenuation measurements. This work proposes to investigate whether artificial eardrums designed with acoustic resonators and dissipative elements are practically able to cover the inter-individual variability of the human tympanic impedance. This capability is verified thanks to Monte Carlo simulations using an artificial eardrum model whose dimensions are constrained in feasible fabrication ranges.

Keywords: earplug, attenuation, tympanic impedance, artificial eardrum

1. Introduction

Acoustical test fixtures (ATFs) are commonly used to assess the insertion loss of hearing protectors. According to standard [1], ATFs must be fabricated with required specifications. For example, ATFs must have an earcanal with dimensions representative of a panel of humans, a head-like shape and must embed an ear simulator mimicking the acoustical behaviour of the inner and middle ear including the eardrum. This ear simulator is designed to simulate the average acoustic tympanic impedance of a panel of humans. Although it is known that the tympanic impedance has small effects on the attenuation for earmuffs, ear simulators are required for the attenuation evaluation of in-ear devices like earplugs [2-3].

Since ear simulators are designed using an average tympanic impedance, the question arises whether the inter-individual variability of the tympanic impedance has an effect on the attenuation evaluation of earplugs. A previous numerical study [4] has demonstrated that the inter-individual variability of the

tympanic impedance observed in the literature can have an effect on the attenuation of an earplug up to 4 kHz. Thus, the use of several artificial eardrums that provide different tympanic impedances could be useful to (i) experimentally confirm that the inter-individual variability of the tympanic impedance has an effect on the earplug attenuation and (ii) propose a manner to consider this inter-individual variability during earplug attenuation measurements.

This paper investigates if artificial eardrums designed with acoustical resonators and dissipative elements could be used to cover the inter-individual variability of the human tympanic impedance observed in the literature. In Section 2, a model of an artificial eardrum is proposed and optimized to fit an average tympanic impedance taken from the literature [5]. Then, the optimized artificial eardrum is fabricated. In Section 3, the prototype artificial eardrum is validated using impedance tube measurements. Its effects on the impedance at the entrance of a realistic earcanal are experimentally investigated using a realistic artificial ear. In Section 4, a Monte Carlo simulation is used to determine if the proposed design of the artificial eardrum is able to cover the inter-individual variability of the human tympanic impedance when varying its dimensions within practical ranges.

2. Artificial eardrum design

2.1 Inter-individual variability and average of the human tympanic impedance

Tympanic impedance can be measured directly in front of the tympanic membrane or, applying a reduced impedance method on a measurement done at a known distance from the eardrum. Both methods include sources of errors. For example, the direct method is hardly applicable to subjects and is always conducted on cadavers. This brings some differences compared to measurements on living humans. Figure 1 presents two sets of data that cover the largest tympanic impedance variability found in the literature [6-7].

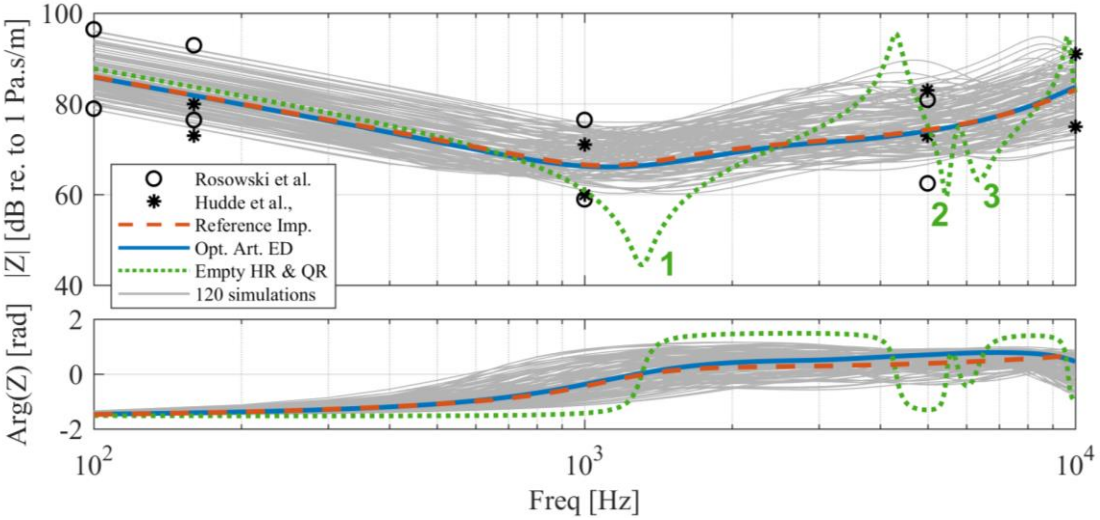

Figure 1: Black circles and stars indicate the extreme tympanic impedance values manually extracted from [6] and [7] respectively. The red dashed line indicates the reference impedance obtained from [5]. Solid blue and dotted green lines indicate respectively the optimized artificial eardrum impedance computed using the analytical model presented in section 2.3 and the artificial eardrum impedance computed with no porous material. Grey lines present 120 among the 10000 artificial eardrum impedances obtained from a Monte Carlo method used to simulate the inter-individual variability of the tympanic impedance observed in the literature (see section 4).

In this study, the variability of the tympanic impedance observed in Figure 1 (black circles and stars) is considered to be mainly due to the tympanic impedance inter-individual variability of the tested panels of subjects. It is assumed that the variability due to experimental or computational errors are smaller than the tympanic impedance differences among subjects.

A tympanic impedance derived from a standardized ear simulator IEC 60318-4 obtained from [5] is also plotted in Figure 1 (dashed red curve). This impedance, considered as an average, is effectively in the midrange of the inter-individual variability obtained with datasets found in the literature and is considered as the reference impedance in the following sections of this paper.

2.2 Concept of the artificial eardrum

Existing ear simulators include various acoustical components like resonators, grids, slits or porous materials used to reproduce the middle and inner ear acoustical behaviour [8-10]. Several studies in the literature have shown that the use of one or two resonators in parallel whose neck apertures are located at the end of the earcanal allows for mimicking the behaviour of a tympanic impedance [5,11]. In this study, it is arbitrarily proposed to design an artificial eardrum using two acoustic resonators (one Helmholtz resonator (HR) and one quarter wavelength resonator (QR)) whose apertures share a common front surface designed to be located at the end of an earcanal as presented in Figure 2. To be able to control the damping in the artificial eardrum, the cavity of the Helmholtz and quarter wavelength resonators can be filled with a sound absorbing porous material.

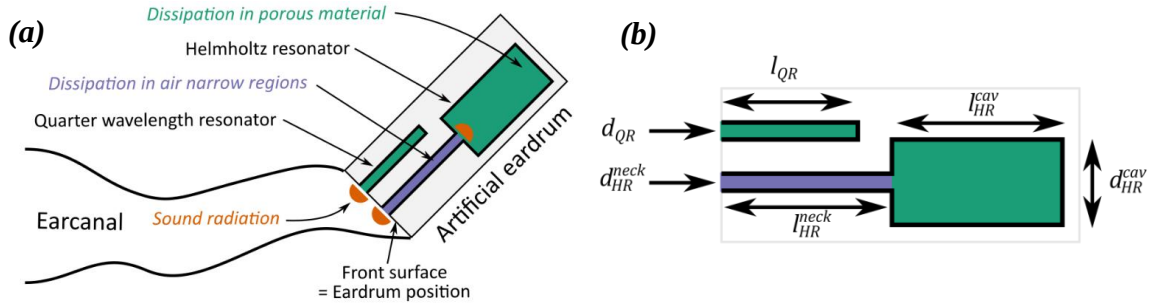

Figure 2: (a) Concept of the artificial eardrum located at the end of an earcanal. Colours represent the sound radiation at resonator apertures (orange), the dissipation in air narrow regions (velvet) and in sound absorbing porous material (green). (b) Notations for the geometrical features of the Helmholtz and quarter wavelength resonators.

2.3 Analytical modelling and optimization

In order to design the artificial eardrum, it is proposed to tune its features (both dimensions and porous material properties) to fit the reference tympanic impedance presented in Section 2.1. For this purpose, an analytical model of the artificial eardrum is developed. The proposed analytical model relies on the plane wave assumption since the resonators' diameters are small with respect to the minimum acoustic wavelength corresponding to the upper frequency limit of interest (approximately 34 mm at 10 kHz). The total acoustic impedance of the artificial eardrum Z is computed using the admittance sum method [12] and depends on the input acoustic impedance of both resonators and on the ratios between the area of their entrance cross-sections and that of the front surface shown in Figure 2. The sound radiation at resonator apertures, represented in orange in Figure 2, is modelled using end corrections [13]. Visco-thermal dissipation due to the sound propagation in air narrow regions and depicted with velvet areas in Figure 2 is modelled using the low reduced frequency method [14]. Visco-thermal dissipation in the porous material symbolized by the green area in Figure 2 is modelled using Miki's model [15].

Then, resonators dimensions and porous materials properties of the model are optimized with the *ga* and *fminsearch* algoritms from Matlab (Mathworks, USA)) in order to fit the analytical impedance of the artificial eardrum with the reference impedance described in Section 2.1. The optimization problem consists in minimizing a cost function equal to the sum on frequencies of the relative errors between the modulus and phase of the reference impedance and of the artificial eardrum impedance. It is performed using 50 points per decade in the frequency range from 100 Hz to 10 kHz. The result of the optimization is illustrated with solid blue lines in Figure 1 and corresponding optimized values are given in Table 1.

For the entire frequency range, the optimized artificial eardrum impedance modulus (solid blue line) agrees well with the reference impedance (red dashed line). The phase of the impedance is less accurate above 2 kHz but remains acceptable since no important phase shift is observed. The impedance of the optimized artificial eardrum is also computed without porous material in both cavities (*i.e.* $\sigma_{abs,HR} = \sigma_{abs,QR} = 0$ N.s.m^{-4}) (green dotted lines in Figure 1). In this case, the resonance frequency of the HR appears at 1310 Hz, its first cavity resonance at 5450 Hz and the resonance of the QR at 6320 Hz (respectively markers 1, 2 and 3 in Figure 1).

Table 1: Optimized parameters of the artificial eardrum.

Variable [Unit]	l_{HR}^{neck} [m]	d_{HR}^{neck} [m]	l_{HR}^{cav} [m]	l_{HR}^{cav} [m]	$\sigma_{abs,HR}$ [Pa.s/m^2]	l_{QR} [m]	d_{QR} [m]	$\sigma_{abs,QR}$ [Pa.s/m^2]
Optimized value	7e-3	1.7e-3	33.1e-3	3.7e-3	40000	12.7e-3	1e-3	31000

2.4 Fabrication of the artificial eardrum

The optimized artificial eardrum was 3D-printed using a Form 2 printer (© Formlabs, USA) and a clear resin (RS-F2-GPCL-04). A miniature microphone (FG-23629-P16 Knowles, USA), not used in this study, was flush mounted in the front surface of the artificial eardrum in order to carry out acoustic pressure measurements at the tympanic membrane position. Figure 3 presents a schematic of the 3D geometrical model of the artificial eardrum together with its physical counterpart. The transversal cut of the 3D model of the artificial eardrum reveals the inner positions of the HR and QR. The back of the HR can be opened in order to fill its cavity with porous material visible in Figure 3(b). This material is a flexible polyurethane foam of airflow resistivity measured between 8000 and 16000 N.s.m^{-4} on 10 mm diameter uncompressed samples.

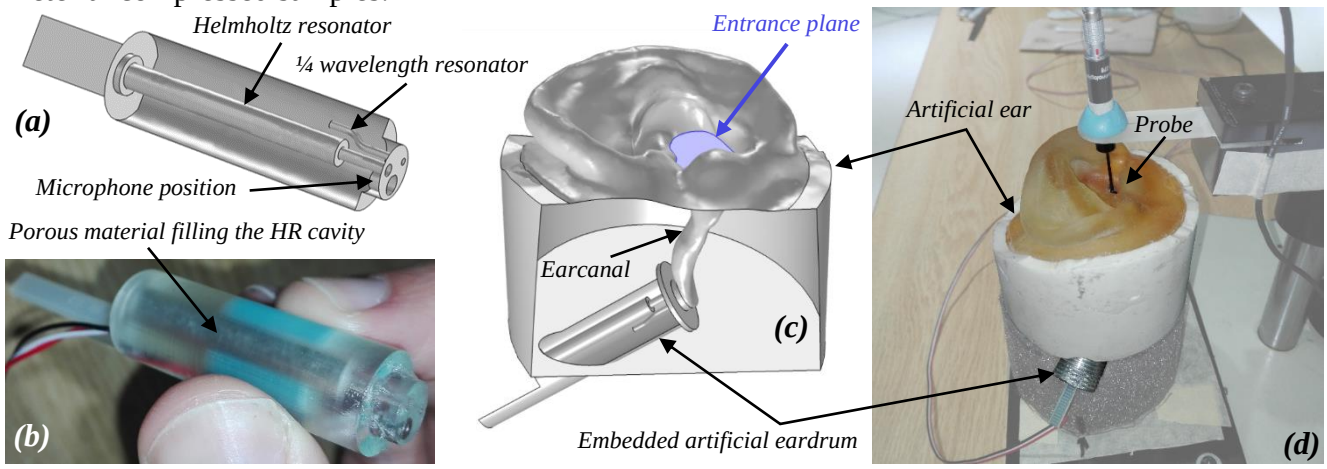

Figure 3: (a) 3D geometrical model of the artificial eardrum and (b) its physical counterpart. (c) 3D modelling of the artificial eardrum embedded in the artificial ear and (d) 1D impedance measurement at the entrance of the artificial ear using a sound intensity probe (see section 3.2).

Two porous material configurations are considered in which the HR cavity is filled firstly with a column of the material roughly fitting its dimensions (referred to as "Abs#1") and secondly with a column of porous material with twice the length of the HR cavity and compressed into it (referred to as "Abs#2"). The exact determination of the airflow resistivity of the porous material filling the HR cavity was challenging due to the material compression and possible leaks along its circumference. Thus, the values of airflow resistivity corresponding to each configuration were obtained by fitting the analytical model to measurements presented in Section 3.1. Configuration "Abs#2" matches the property of the porous material obtained via the optimization presented in Section 2.3. Configuration "Abs#1" is used to investigate the effect of a less damped impedance of the artificial eardrum. Since the optimized dimensions of the

QR are very small (see Table 1), it was not possible to fill this cavity with the porous material. Thus, measurements were conducted with an empty QR.

3. Testing of the prototype artificial eardrum

3.1 Characterisation and validation of the artificial eardrum impedance

The prototype artificial eardrum was used to experimentally validate the analytical model described in Section 2.3 and to calibrate the airflow resistivity of porous materials used in the configurations described in Section 2.4. To these purposes, the surface impedance of the physical artificial eardrum was measured in an impedance tube of diameter $d_{IT} = 29\ mm$. In this tube, the lower and upper cut off frequencies are approximately 860 and 6900 Hz. For the validation of the analytical model, two artificial eardrum configurations were tested: (1) closed HR and QR (referred to as "Rigid") and (2) open but empty resonators (referred to as "NoAbs"). The first configuration, equivalent to an impedance tube with a rigid ended termination, is used to ensure that the analytical model catches very simple surface impedance. The second one is used to validate the modelling of the resonators and of the dissipation in air narrow regions. The two configurations (3) Abs#1 and (4) Abs#2 described in Section 2.4 are also tested in the impedance tube in order to calibrate the airflow resistivity of the porous materials in both cases. This is necessary to verify that the porous material used in configuration Abs#1 corresponds to the optimized value of the HR cavity airflow resistivity given in Table 1.

From a practical point of view, the tested artificial eardrum was embedded in a sample holder specially designed to fit in the impedance tube and adjusted with an o-ring to ensure a perfect acoustic seal. To correctly account for evanescent modes in the impedance tube, end corrections depending on the area ratio between the entrance of resonators and the tube cross-section are added to the analytical model of the artificial eardrum. For practical reasons, the impedance inside the tube was measured 1 mm ahead the location of the artificial eardrum. This 1 mm thick air layer was also added to the analytical model. Results for the artificial eardrum impedance measurements are shown in Figure 4.

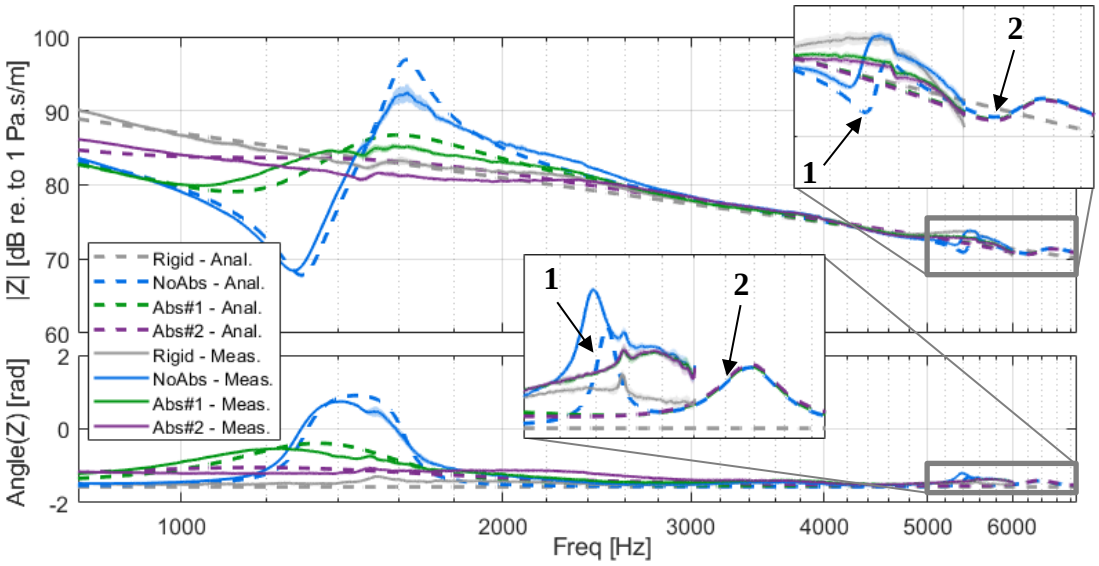

Figure 4: Surface impedances measured (plain lines) and computed (dashed lines) 1 mm in front of the artificial eardrum in an impedance tube for the "Rigid" (grey), "NoAbs" (blue), "Abs#1" (green) and "Abs#2" (purple) configurations described in Sections 2.4 and 3. Numbers 1 and 2 respectively point out the first HR and QR cavity resonances computed analytically.

Solid and dashed lines correspond respectively to measured and analytically computed impedances. Shaded regions around solid lines correspond to the average of three measurements plus or minus one

standard deviation. Grey and blue lines correspond respectively to the two measurements configurations referred to as "Rigid" and "NoAbs". These plots show that the modulus level and phase of the acoustical impedance are well predicted by the analytical model. Blue lines indicate that the Helmholtz resonance occurs at 1286 Hz in the measurement and correspond to the resonance computed using the analytical model. The first cavity resonance of the HR indicated by marker 1 in zoom boxes of Figure 4 and observed around 5300 Hz is also well predicted by the model. The computed QR resonance indicated by marker 2 in zoom boxes of Figure 4 appears around 6200 Hz. This theoretical frequency is slightly above the highest measured frequency. Nevertheless, since a good agreement is obtained between measured and computed impedances, the analytical model of the artificial eardrum proposed in this paper can be used with a good confidence for artificial eardrum design. In Figure 4, green and purple lines correspond respectively to the two configurations referred to as "Abs#1" and "Abs#2" in Section 2.4. Results for the fitting of the airflow resistivity of the porous material filling the HR cavity in these configurations are $\sigma_{Abs\#1,HR} = 8000$ Pa.s.m^{-2} and $\sigma_{Abs\#2,HR} = 40000$ Pa.s.m^{-2}. It is noteworthy that configuration Abs#2 corresponds to the material properties found with the optimization described in Section 2.3.

3.2 Effects of the artificial eardrum at the entrance of a realistic artificial earcanal

Since the artificial eardrum aims to mimic a real tympanic impedance, it is embedded in an artificial ear in order to investigate the basic effects it may have on the acoustical behaviour of the latter. This is achieved using impedance measurements at the entrance of an artificial ear of realistic geometry to which the artificial eardrum is connected. This artificial ear, shown in Figure 3(c-d), was reconstructed from magnetic resonance images of the ear of a human subject [16]. It consists of a truncated region including an earcanal cavity surrounded by synthetic soft tissues and bones. The artificial eardrum is inserted from the back of the artificial ear using an aluminium insert screwed into the bony part up to the location of the tympanic membrane, and acoustically sealed using an o-ring. Thus, the front surface of the artificial eardrum has an anatomically correct position and orientation in the artificial earcanal (see Figure 3(c)).

Impedances were measured in a plane, referred to as the entrance plane of the artificial earcanal (see Figure 3(c)), using a one-dimensional sound intensity probe (©-Microflown technologies, Netherlands) shown in Figure 3(d). The measurements were performed in a 211 m^3 reverberant room using white noise delivered by four Mackie HD1531 loudspeakers and have been repeated 3 times to test the reproducibility. Four artificial eardrums corresponding to configurations "Rigid", "NoAbs", "Abs#1" and "Abs#2" described in Section 3.1 were successively tested. The measured impedances are presented in Figure 5.

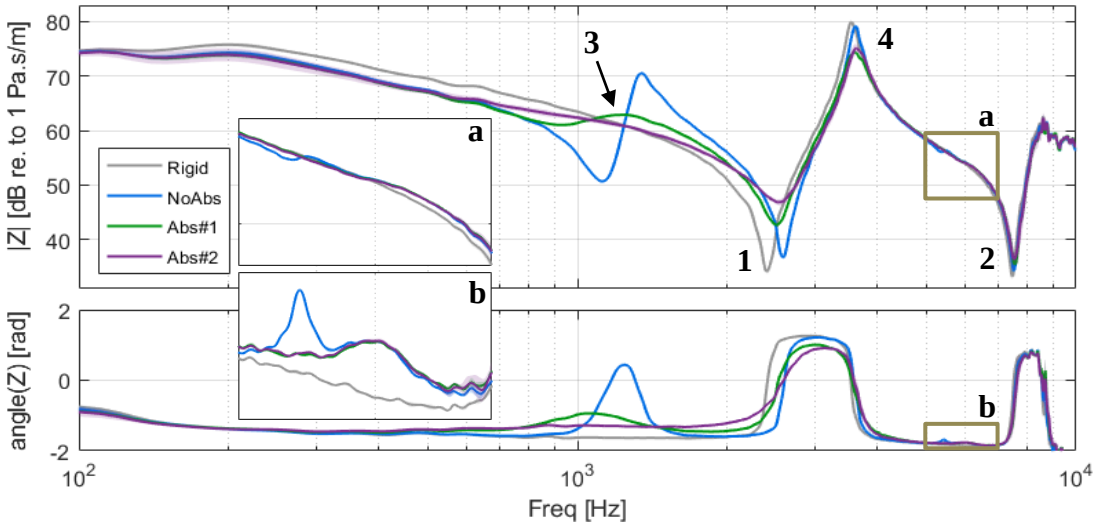

Figure 5: Measured impedances at the entrance of a realistic artificial earcanal for four artificial eardrum configurations referred to as "Rigid" (gray), "NoAbs" (blue), "Abs#1" (green) and "Abs#2" (purple). Rectangles (a) and (b) correspond to zoom boxes of the modulus (top) and the phase (bottom) of measured impedances. Transparent regions correspond to the standard deviation of measurements.

The impedance modulus measured in the "Rigid" configuration exhibits two minima (markers 1 and 2 in Figure 5) corresponding to the earcanal resonances at 2400 Hz and 7460 Hz. The flat region of the impedance modulus below 200 Hz is suspected to be due to the disturbance of the acoustic field by the sound intensity probe used for measurement [5]. When the artificial eardrum is used in the "NoAbs" configuration, the presence of the empty HR shifts the first earcanal resonance to higher frequencies (2580 Hz). The resonance of the HR itself is shifted to lower frequencies (1120 Hz) compared to the frequency measured in Section 3. The first cavity resonance of the HR and the resonance of the QR are localized around 5500 Hz. Their effects observed in the zoom boxes in Figure 5 are hardly visible on the impedance. This is due to the fact that the impedance is not measured on the front surface of the artificial eardrum but at the entrance of the artificial earcanal. The use of porous material (configurations "Abs#1" and "Abs#2") has two main effects on the impedance at the entrance of the earcanal. Firstly, the resonance of the HR is damped resulting in a bump around 1 kHz (see marker 3 in Fig. 5) very similar to those described in Figure 12 in [8] and observed in Figure 2 in [17] for example. This trend is attributed to the effect of the eardrum and middle ear [8]. Depending on the subject, the amplitude of the bump can vary as it is the case for configurations "Abs#1" and "Abs#2" (see Fig. 2(a1) in [17] for example). The second effect of the porous material is to damp the first resonance and anti-resonance of the earcanal (markers 1 and 4 in Figure 5). Indeed, in human earcanals these (anti-)resonances are not as sharp as in a rigid earcanal [10]. The higher the airflow resistivity, the more damped the resonance. These results show that the artificial eardrum has the expected effects on the impedance at the entrance of a realistic earcanal.

4. Capability of the artificial eardrum to cover the inter-individual variability of the human tympanic impedance

In order to determine whether the proposed artificial eardrum is able to cover the inter-individual variability of the tympanic impedance observed in the literature, a Monte Carlo method was used in combination with the analytical model of the artificial eardrum presented in Section 2.3. Ten thousand random sets of the resonator's dimensions were generated assuming a uniform distribution around the optimized values of the artificial eardrum given in Table 1. The interval of the uniform distribution was arbitrarily set to +/-35% of the nominal value for each optimized dimension since these limits enable to cover a reasonable part of the tympanic impedance variability. Note that the obtained sets of dimensions can be achieved from a manufacturing point of view. Then, the artificial eardrum analytical model was used to compute the tympanic impedance for each set of dimensions. Properties of the porous materials were kept to their optimized values given in Table 1 for all simulations. One hundred and twenty impedances among the ten thousand computed during simulation are presented in Figure 1. Results of the Monte Carlo simulation reveal that, applying a +/-35% random variation of the optimized dimensions, artificial eardrums are theoretically able to cover the tympanic impedance inter-individual variability observed in the literature. However, the difficulty in filling the QR and in obtaining porous material samples with the desired airflow resistivity makes some artificial eardrum configurations hard to fabricate. Other designs of the artificial eardrum could be proposed to fulfil these limitations.

5. Conclusion

In order to investigate the necessity to account for the inter-individual variability of the human tympanic impedance when using ATFs for earplug attenuation assessment, the design of artificial eardrums was addressed in this paper. Firstly, the modelling and design of an artificial eardrum mimicking the overall behaviour of a human eardrum, middle and inner ears were presented. The proposed analytical modelling was performed using acoustical resonators whose impedances were optimized to fit a reference impedance. A prototype artificial eardrum was fabricated and validated using impedance tube measurements also used to calibrate the porous material properties filling the HR cavity. The overall effects

of the prototype artificial eardrum embedded in a realistically shaped earcanal were experimentally investigated using measurements with a sound intensity probe. It was found that the main effects of the artificial eardrum on the acoustic behaviour of the outer earcanal (*i.e.* to damp the earcanal resonances and anti-resonances and to account for the eardrum and middle ear resonance) were observed in the same manner as in the literature. Secondly, it was shown that the proposed artificial eardrum concept is theoretically able to cover the inter-individual variability of the tympanic impedance observed in the literature by modifying its dimensions in practically feasible ranges. The difficulty in obtaining porous material samples with the desired airflow resistivity and in using them to fill small cavities is the main limitation of this work.

REFERENCES

1 ANSI/ASA S3.36-2012, Specification for a manikin for simulated in-situ airborne acoustic measurements, American National Standard Institute, Inc., (2012).

2 Schroeter, J., Els, H., On basic research towards an improved artificial head for the measurement of hearing protectors", *Acta Acustica united with Acustica*, **50** (4), 250-260, (1982).

3 Bockstael, A., de Greve, B., Van Renterghem, T., Botteldooren, D., D'Haenens, W., Keppler, H., Maes, L., Philips, B., Swinnen, F., Vinck, B., Verifying the attenuation of earplugs in situ: method validation using artificial head and numerical simulations, *Journal of the Acoustical Society of America*, **124** (2), 973-81, (2008).

4 Benacchio, S., Luan, Y., Doutres, O., Sgard, F., Influence de l'impédance tympanique sur la perte par insertion de protecteurs auditifs intra-auriculaires, *Proceedings of the 16^{tième} Congrès Français d'Acoustique (CFA)*, Marseille, France, 11-15 April, (2022).

5 Luan, Y., Sgard, F., Benacchio, S., Nélisse, H., Doutres, O., A transfer matrix model of the IEC 60318-4 ear simulator: Application to the simulation of earplug insertion loss, *Acta Acustica united with Acustica*, **105** (6), 1258-1268, (2019).

6 Rosowski, J. J., Davis, P. J., Merchant, S. N., Donahue, K. M., Coltrera, M. D., Cadaver middle ears as models for living eras: comparisons of middle ear input immittance, *Ann. Otol. Rhinol. Laryngol.*, **99** (5.1), 403-12, (1990).

7 Hudde, H., Engel, A., Measuring and modeling basic properties of the human middle ear and ear canal. Part III: Eardrum impedances, transfer functions and model calculations, *Acta Acustica united with Acustica*, **84** (6), 1091-1108, (1998).

8 Brüel & Kjær, High-frequency head and torso simulator type 5128 family, Brüel & Kjær product data, (2019).

9 Jonsson, S., Liu, B., Schuhmacher, A., Nielsen, L., Simulation of the IEC 60711 occluded ear simulator, *Proceedings of the 116th Convention of the Audio Engineering Society*, Berlin, Germany, 8-11 May, (2004).

10 Stinson, M. R., The spatial distribution of sound pressure within scaled replicas of the human ear canal, *Journal of the Acoustical Society of America*, **78** (5), 1596-602, (1985).

11 Gardner, M. B., Hawley, M. S., Network representation of the external ear, *Journal of the Acoustical Society of America*, **52** (6), 1620-8, (1972).

12 Verdière, K., Panneton, R., Elkoun, S., Comparison between parallel transfer matrix method and admittance sum method, *Journal of the Acoustical Society of America*, **136** (2),(2014).

13 Mechel, F. P., *Formulas of acoustics*, Publisher: Springer, Editor: F. P. Mechel, (2008).

14 Kampinga, W. R., *Viscothermal acoustics using finite elements – Analysis tools for engineers*, PhD thesis, University of Twente, (2010).

15 Miki, Y., Acoustical properties of porous materials – Modifications of Delany-Bazley models, *Journal of the Acoustical Society of Japan*, **11** (1), 19-24, (1990).

16 Benacchio, S., Doutres, O., Le Troter, A., Varoquaux, A., Wagnac, E., Callot, V., Sgard, F., Estimation of the ear canal displacement field due to in-ear device insertion using a registration method on a human-like artificial ear, *Hearing Research*, **365**, 16-27, (2018).

17 Withnell, R. H., Gowdy, L. E., An analysis of the acoustic input impedance of the ear, *Journal of the Association for Research in Otolaryngology*, **14** (5), 611-22, (2013).